

Performance of magnetic fluid based circular step bearings

G.M. Deheri*, H.C. Patel**, Rakesh M. Patel***

*Sardar Patel University, Vallabh Vidyanagar – 388 120 Gujarat, India, E-mail: gmdeheri@rediffmail.com

**Government Engineering College, Chandkheda, Gandhinagar, Gujarat, India, E-mail: prof_himanshu@rediffmail.com

***Gujarat Arts and Science College, Ahmedabad – 380 006 Gujarat State, India, E-mail: jrmpatel@rediffmail.com

1. Introduction

Elwell and Sternlicht [1] analyzed the performance of a thrust bearing theoretically as well as experimentally. Dowson [2] studied the inertia effects in hydrostatic thrust bearings. Majumdar and Ghosh [3] considered externally pressurized oil lubricated rectangular thrust bearing. Stiffness and damping characteristic of compensated thrust bearings were dealt with by Ghosh and Majumdar [4]. Majumdar [5] studied the performance of an oil lubricated circular step bearing. Lin [6] investigated the performance of an externally pressurized circular step bearings lubricated with couple stress fluids. Lin and Chiang [7] discussed the effects of surface roughness and rotational inertia on the optimal stiffness of thrust bearings.

Verma [8] and Bhat and Deheri [9] investigated the performance of squeeze film behavior between porous annular plates and observed that its performance with magnetic fluid lubricant was much better than with conventional lubricant. Further, Bhat and Deheri [10] considered a magnetic fluid based squeeze film in curved porous circular plates. Recently, Patel and Deheri [11] investigated the behavior of a magnetic fluid based squeeze film between porous circular plates with a concentric circular pocket.

Here we seek to study the configuration of Majumdar [5] in the presence of a magnetic fluid.

2. Analysis

Normally, the following assumptions are made to obtain the load capacity, flow requirement and frictional power loss.

(i) The recess is deep enough for the pressure in it to be uniform.

(ii) The bearing has low rotational velocity and its effect is neglected for the pressure development.

The configuration of the bearing system is shown in Fig. 1 wherein, a thrust load w is applied and the bearing supports the load without metal to metal contact. The load w is supported by the fluid within the pocket and land. The fluid escapes radially through the restriction by a land or sill around the recess. A magnetic fluid based film is formed with film thickness h . We assume axially symmetric flow of magnetic fluid under an oblique magnetic field \bar{H} whose magnitude H is a function of r vanishing at $r = r_i$ and r_0 . Then the associated Reynolds equation [5] yields the pressure induced flow for a circular step bearing as

$$Q = -\frac{h^3}{12\eta} 2\pi r \frac{d}{dr} (p - 0.5\mu_0 \bar{\mu} H^2) \quad (1)$$

where μ_0 is the permeability of free space; $\bar{\mu}$ is magnetic susceptibility; η is the absolute viscosity of the fluid and

$$H^2 = (r - r_i)(r_0 - r); \quad r_i \leq r \leq r_0$$

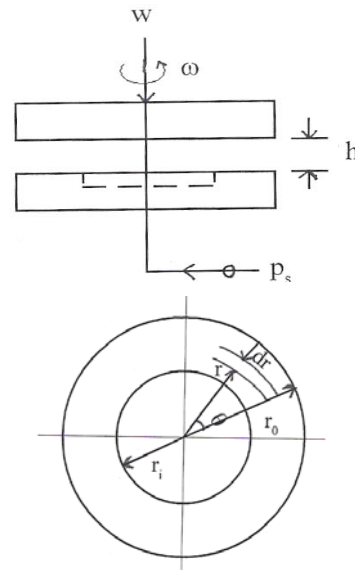


Fig. 1 Configuration of the bearing system

In view of the boundary conditions

$$r = r_0; \quad p = 0 \quad \text{and} \quad r = r_i; \quad p = p_s$$

(the supply pressure) the governing equation for the film pressure p is obtained as

$$p = 0.5\mu_0 \bar{\mu} H^2 + p_s \frac{\ln\left(\frac{r}{r_0}\right)}{\ln\left(\frac{r_i}{r_0}\right)} \quad (2)$$

wherein

$$p_s = \frac{6Q\eta}{\pi h^3} \ln\left(\frac{r_0}{r_i}\right) \quad (3)$$

Hence the dimensionless pressure is obtained as

$$P = -\frac{h^3 p}{\eta h \pi r_0^2} = \frac{\mu^* (R - \alpha)(1 - R)}{2\pi} + \frac{P_s \ln R}{\ln \alpha} \quad (4)$$

where the non dimensional quantities are

$$\mu^* = -\frac{h^3 \mu_0 \bar{\mu}}{\eta \dot{h}}; R = \frac{r}{r_0}; \alpha = \frac{r_i}{r_0}; P_s = -\frac{h^3 p_s}{\eta \dot{h} \pi r_0^2}$$

The load carrying capacity is calculated by integrating the pressure, which takes the form

$$W = \frac{\pi \mu_0 \bar{\mu}}{12} (r_0 + r_i) (r_0 - r_i)^3 + \frac{\pi p_s (r_0^2 - r_i^2)}{2 \ln(r_0 / r_i)} \quad (5)$$

Then the load carrying capacity in dimensionless form is calculated as

$$\begin{aligned} \bar{W} &= -\frac{h^3 W}{\eta \dot{h} \pi^2 r_0^4} = \\ &= \frac{\mu^* (1 + \alpha)(1 - \alpha)^3}{12\pi} + \frac{P_s (1 - \alpha^2)}{2 \ln(1 / \alpha)} \end{aligned} \quad (6)$$

Lastly, the response time Δt , to reach a film thickness h_2 at t_2 starting from an initial film thickness h_1 at t_1 is given by

$$\Delta t = \frac{\eta \pi^2 r_0^4 \bar{W}}{2W} \left(\frac{1}{h_2^2} - \frac{1}{h_1^2} \right) \quad (7)$$

Now the response time in dimensionless form becomes

$$\bar{\Delta t} = \frac{W h^2 \Delta t}{\eta \pi^2 r_0^4} = \frac{\bar{W}}{2} \left(\frac{1}{\bar{h}_2^2} - \frac{1}{\bar{h}_1^2} \right) \quad (8)$$

where $\bar{h}_1 = \frac{h_1}{h}$ and $\bar{h}_2 = \frac{h_2}{h}$.

3. Results and discussion

The pressure distribution, load carrying capacity and response time are obtained from equations (4), (6) and (8) respectively. It is clear that these performance characteristics depend upon various parameters such as magnetization μ^* and radii ratio α while it is needless to say that these performance characteristic depend upon supply pressure p_s . From equations (3) and (5) it is seen that $W \propto p_s$

and $p_s \propto \frac{Q}{h^3}$. Therefore for constant flow rate the load capacity increases as the film thickness decreases. Hence the bearing is self compensating provided the flow rate is held constant. It is observed from equations (4) and (6) that the dimensionless pressure P and load carrying capacity \bar{W} get increased by

$$\frac{\mu^* (R - \alpha)(1 - R)}{2\pi}$$

and

$$\frac{\mu^* (1 + \alpha)(1 - \alpha)^3}{12\pi}$$

respectively. Besides, the increase in the response time is also

$$\frac{\mu^* (1 + \alpha)(1 - \alpha)^3}{24\pi}$$

Thus, it is easily observed that the magnetization parameter μ^* has considerable positive effect on the performance of the bearing system.

Fig. 2 presents the variation of the load carrying capacity with respect to the magnetization parameter μ^* for various values of the radii ratio α . In Fig. 3 we have the distribution of the load carrying capacity with respect to radii ratio α for various values of magnetization parameter μ^* . Fig. 4 describes the variation of the load carrying capacity with respect to the magnetization parameter μ^* for various values of the supply pressure P_s [12]. Fig. 5 depicts the distribution of the load carrying capacity with respect to the supply pressure P_s for various values of the magnetization parameter μ^* . Fig. 6 gives the variation of load capacity with respect to the supply pressure P_s for different values of the radii ratios while in Fig. 7 one finds the distribution of the load carrying capacity with respect to the radii ratio α for different values of supply pressure P_s . It is observed from Figs. 2 and 4 that the load carrying capacity significantly increases with increasing values of magnetization parameter μ^* . Figs. 3 and 7 make it clear that increasing values of radii ratio α cause decreasing load carrying capacity. It is obvious from Figs. 5 and 6 that supply pressure increases the load carrying capacity. Further, it is observed from Figs. 8-13 that the response time follows the trends of the load carrying capacity.

Table 1

Variation of load carrying capacity with respect to μ^* and α for $P_s = 1$

α/μ^*	0.00000000	0.00100000	0.01000000	0.10000000	1.00000000
0.25000000	0.64982548	0.64996354	0.65120606	0.66363131	0.78788375
0.35000000	0.460609457	0.460706518	0.461580062	0.470315506	0.557669944
0.45000000	0.318404944	0.318468101	0.319036519	0.32472069	0.38156241
0.55000000	0.208495654	0.208532632	0.208865429	0.212193407	0.245473181
0.65000000	0.124388567	0.124407088	0.124573774	0.126240634	0.142909237

Table 2

Variation of load carrying capacity with respect to μ^* and P_s for $\alpha = 0.35$

P_s/μ^*	0.00000000	0.00100000	0.01000000	0.10000000	1.00000000
1.00000000	0.46060946	0.46070652	0.46158006	0.47031551	0.55766994
1.50000000	0.69091419	0.69101125	0.69188479	0.70062023	0.78797467
2.00000000	0.92121891	0.92131597	0.92218952	0.93092496	1.01827940
2.50000000	1.15152364	1.15162070	1.15249425	1.16122969	1.24858413
3.00000000	1.38182837	1.38192543	1.38279898	1.39153442	1.47888886

Table 3

Variation of carrying capacity with respect to α and P_s for $\mu^* = 0.01$

P_s/α	0.25000000	0.35000000	0.45000000	0.55000000	0.65000000
1.00000000	0.65120606	0.46158006	0.31903652	0.20886543	0.12457377
1.50000000	0.97611881	0.69188479	0.47823899	0.31311326	0.18676806
2.00000000	1.30103155	0.92218952	0.63744146	0.41736108	0.24896234
2.50000000	1.62594429	1.15249425	0.79664393	0.52160891	0.31115662
3.00000000	1.95085703	1.38279898	0.95584641	0.62585674	0.37335091

Table 4

Variation of response time with respect to μ^* and α for $P_s = 1$

α/μ^*	0.00000000	0.00100000	0.01000000	0.10000000	1.00000000
0.25000000	0.18276342	0.18280225	0.18315171	0.18664631	0.22159231
0.35000000	0.12954641	0.12957371	0.12981939	0.13227624	0.15684467
0.45000000	0.08955139	0.08956915	0.08972902	0.09132769	0.10731443
0.55000000	0.05863940	0.05864980	0.05874340	0.05967940	0.06903933
0.65000000	0.03498428	0.03498949	0.03503637	0.03550518	0.04019322

Table 5

Variation of response time with respect to μ^* and P_s for $\alpha = 0.35$

P_s/μ^*	0.00000000	0.00100000	0.01000000	0.10000000	1.00000000
1.00000000	0.12954641	0.129573708	0.129819392	0.132276236	0.156844672
1.50000000	0.194319615	0.194346913	0.194592597	0.197049441	0.221617877
2.00000000	0.25909282	0.259120118	0.259365802	0.261822646	0.286391082
2.50000000	0.323866025	0.323893323	0.324139007	0.326595851	0.351164286
3.00000000	0.388639229	0.388666528	0.388912212	0.391369056	0.415937491

Table 6

Variation of response time with respect to α and P_s for $\mu^* = 0.01$

P_s/α	0.25000000	0.35000000	0.45000000	0.55000000	0.65000000
1.00000000	0.18315171	0.12981939	0.08972902	0.05874340	0.03503637
1.50000000	0.27453341	0.19459260	0.13450472	0.08806310	0.05252852
2.00000000	0.36591512	0.25936580	0.17928041	0.11738280	0.07002066
2.50000000	0.45729683	0.32413901	0.22405611	0.14670251	0.08751280
3.00000000	0.54867854	0.38891221	0.26883180	0.17602221	0.10500494

In addition, this article makes it clear that in the absence of μ^* the results contained in Majumdar [5] are obtained. A comparison shows that magnetization parameter μ^* significantly enhances the performance of the bear-

ing system. Thus, the performance of the bearing system can be enhanced considerably by choosing suitable values of the magnetization parameter, radii ratio and supply pressure.

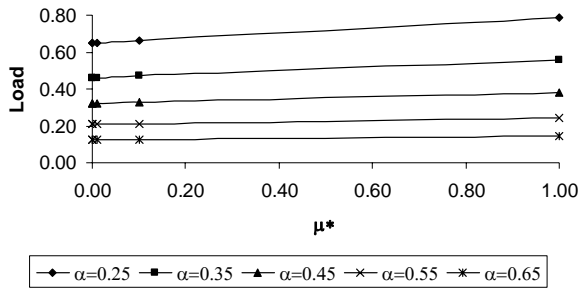


Fig. 2 Variation of load carrying capacity with respect to μ^* for $P_s = 1$

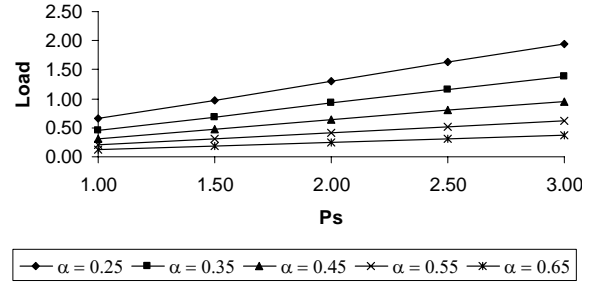


Fig. 6 Variation of load carrying capacity with respect to P_s for $\mu^* = 0.01$

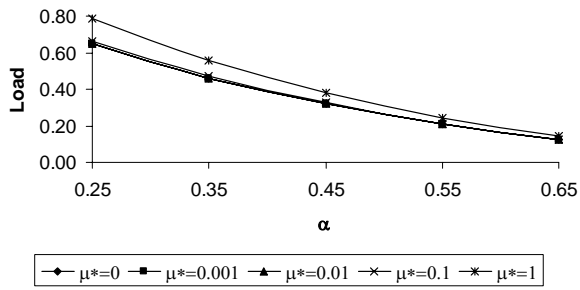


Fig. 3 Variation of load carrying capacity with respect to α for $P_s = 1$

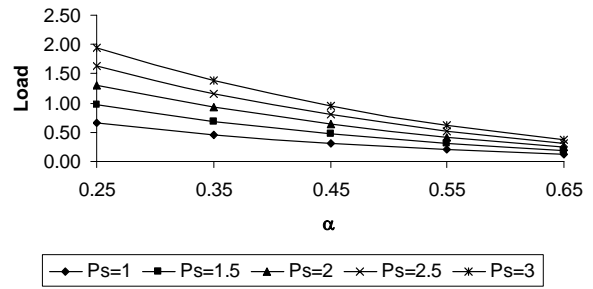


Fig. 7 Variation of load carrying capacity with respect to α for $\mu^* = 0.01$

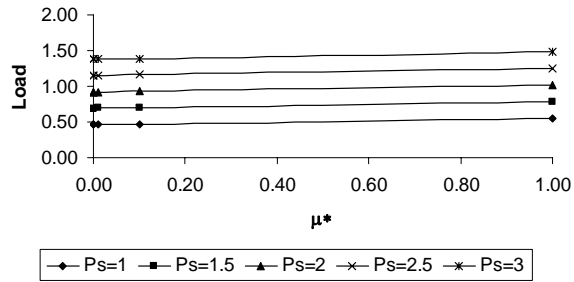


Fig. 4 Variation of load carrying capacity with respect to μ^* for $\alpha = 0.35$

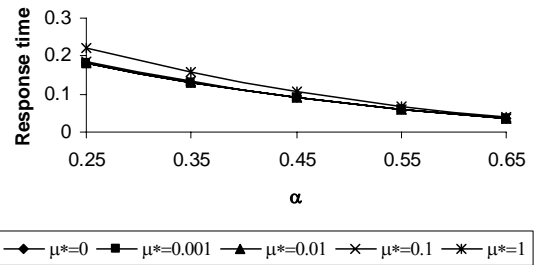


Fig. 8 Variation of response time with respect to α for $P_s = 1$

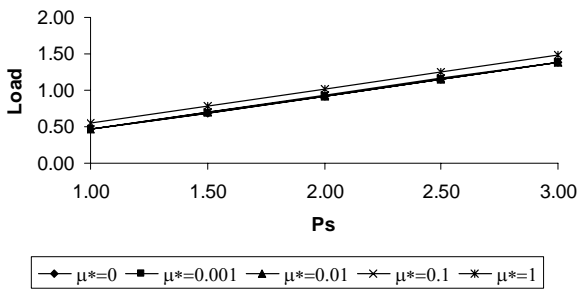


Fig. 5 Variation of load carrying capacity with respect to P_s for $\alpha = 0.35$

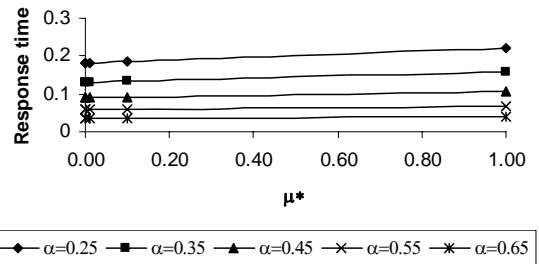


Fig. 9 Variation of response time with respect to μ^* for $P_s = 1$

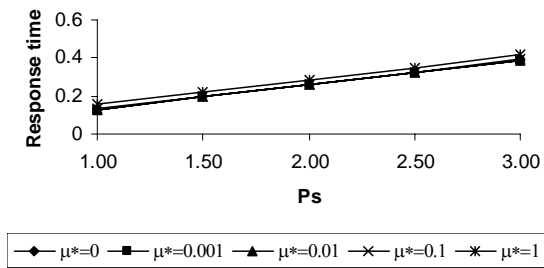


Fig. 10 Variation of response time with respect to P_s for $\alpha = 0.35$

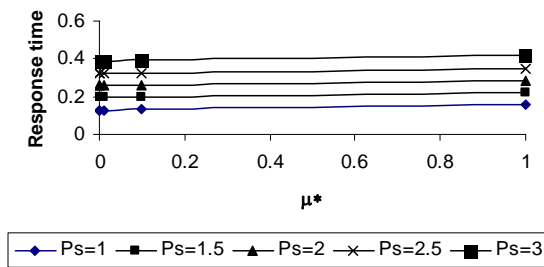


Fig. 11 Variation of response time with respect to μ^* for $\alpha = 0.35$

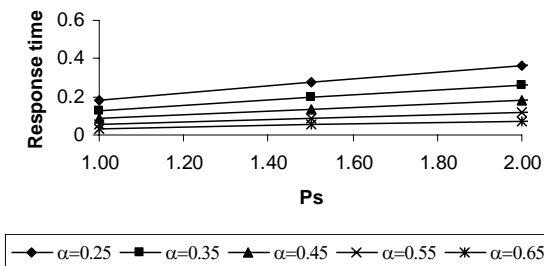


Fig. 12 Variation of response time with respect to P_s for $\mu^* = 0.01$

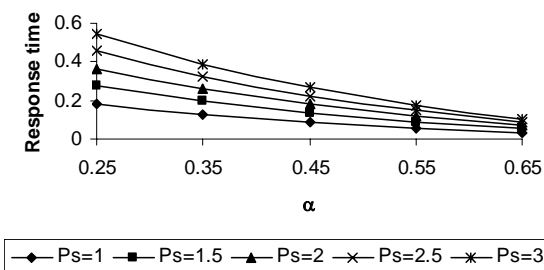


Fig. 13 Variation of response time with respect to α for $\mu^* = 0.01$

References

1. **Elwell, R.C., Sternlicht, B.** Theoretical and experimental analysis of hydrostatic thrust bearings. -J. Basic Engg., Trans. ASME, D, 1960, 82, p.505-512 .
2. **Dowson, D.** Inertia effects in hydrostatic thrust bearings.-J. Basic Engg., Trans. ASME, D, 1961, 83, p.227.
3. **Majumdar, B.C., Ghosh, B.** Load and flow parameters of externally pressurized oil-lubricated rectangular thrust bearings.-M.E. Division, The Instn. of Engrs. (1), 1970, 50, p.253-257.
4. **Ghosh, M.K., Majumdar, B.C.** Dynamic stiffness and damping characteristics of compensated hydrostatic thrust bearings.-J. Lub. Tech., Trans. ASME, F, 1982, 104, p.491-496.
5. **Majumdar, B.C.** Introduction to Tribology of Bearings.-Wheeler Publisher, Wheeler Co. Ltd, 1985.
6. **Lin, J.R.** Static and dynamic characteristics of externally pressurized circular step thrust bearings lubricated with couple stress fluids. -Tribology International, 32,207-216.(SCI)(NSC-88-2212-E-0253-001V), 1999.
7. **Lin, J.R., Chinang, C.F.** Effects of surface roughness and rotational inertia on the optimal stiffness of hydrostatic thrust bearings.-Int. J. of Applied Mechanics and Engineering, 2002, 7, No4, p.1247-1261.
8. **Verma, P.D.S.** Magnetic fluid based squeeze film. -Int. J. of Engineering Sciences, 1986, 24, p.395-401.
9. **Bhat, M.V., Deheri, G.M.** Squeeze film behavior in porous annular disks lubricated with magnetic fluid. -Wear, 1991, 151, p.123-128.
10. **Bhat, M.V., Deheri, G.M.** Magnetic fluid based squeeze film in curved porous circular disks.-J. of Magnetism and Magnetic Material, 1993, 127, p.159-162.
11. **Patel, R.M., Deheri, G.M.** Magnetic fluid based squeeze film behavior between rotating porous circular plates with a concentric circular pocket and surface roughness effects.-Int. J. of Applied Mechanics and Engineering, 2003, 8, No2, p.271-277.
12. **Ajwaliya, M.B.** Behavior of squeeze films between two curved plates, Dissertation (S.P. University, Vallabh Vidhyanagar), 1984.

G.M. Deheri, H.C. Patel, Rakesh M. Patel

MAGNETINIŲ SKYSČIŲ POVEIKIU PAGRĮSTOS ŽIEDINIŲ ATRAMINIŲ GUOLIŲ SAVYBĖS

Reziumė

Darbe tiriama magnetinių skysčių savybėmis pagrįstas žiedinio atraminio guolio darbas. Sprendžiant Reindoldso lygtį ribinėmis sąlygomis, nustatomas slėgio pasiskirstymas, kurio pagalba apskaičiuojama guolio keliamoji galia ir reakcijos trukmė. Skaičiavimo rezultatai pateikti grafiškai. Tyrimas rodo, kad tokia guolių sistema gerokai padidina magnetinių skysčių pritaikomumą. Pastebėta, kad guolio žiedų spindulių santykis turi didelę įtaką guolių sistemos veikimui. Guolių sistemos efektyvumą galima esmingai padidinti, parenkant tinkamas įmagnetinimo parametrų vertes, spindulių santykį ir tinkamą slėgį.

G.M. Deheri, H.C. Patel, Rakesh M. Patel

PERFORMANCE OF MAGNETIC FLUID BASED CIRCULAR STEP BEARINGS

S u m m a r y

Efforts have been made to analyze the performance of a magnetic fluid based circular step bearing. The concerned Reynolds equation is solved with appropriate boundary conditions to obtain the pressure distribution which in turn, is used to get the load carrying capacity leading to the calculation of response time. Results are presented graphically. This investigation reveals that the performance of the bearing system gets enhanced considerably owing to the presence of the magnetic fluid. Further, it is observed that the radii ratio has a strong effect on the performance of the bearing system. In addition, this investigation makes it clear that a performance of the bearing system can be enhanced substantially by choosing suitable values of the magnetization parameter, radii ratio and the supply pressure.

Г.М. Дехери, Х.С. Пател, Ракеш М. Пател

СВОЙСТВА КОЛЬЦЕВЫХ ОПОРНЫХ ПОДШИПНИКОВ ОСНОВАННЫХ НА ДЕЙСТВИИ МАГНИТНОЙ ЖИДКОСТИ

Р е з ю м е

Работа посвящена исследованию свойств работы кольцевых опорных подшипников, основанных на действии магнитной жидкости. При решении уравнения Рейнолдса, применяя граничные условия, определяется распределение давления, при помощи которого рассчитывается несущая нагрузка подшипника и время реакции. Результаты расчетов представлены графически. Исследования показывают, что такая система подшипников значительно увеличивает приспособляемость магнитных жидкостей. Установлено, что соотношение радиусов подшипников значительно влияет на работу подшипниковой системы. Выполненные исследования объясняют, что эффективность подшипниковой системы можно значительно увеличить, подбирая соответствующие значения параметров намагничивания, соотношение радиусов и соответствующее давления.

Received July 14, 2005